Nigerian Journal of Engineering Science Research (NIJESR).
Copyright@ Department of Mechanical Engineering, Gen. Abdusalami Abubakar College of Engineering, Igbinedion University, Okada, Edo State, Nigeria.
ISSN: 2636-7114
Journal Homepage: https://nijesr.iuokada.edu.ng/

Development and Performance Evaluation of a Motorized Cassava Dough Processing Machine

[1]Gbabo Agidi, [2]*Gana Ibrahim Mohammed., [3]Thomas, V.A., [4]Osatola, O.D., and [5]Musa, I.S.

[1]*Department of Agricultural &Bioresources Engineering, Federal University of Technology, Minna, Niger State, Nigeria,*
agagididis@yahoo.com

[2]*Department of Agricultural & Bio-environmental Engineering, Federal Polytechnic Bida, Niger State, Nigeria,*
ganaibro74@yahoo.com

[3] *Department of Agricultural &Bioresources Engineering, Federal University of Technology Minna, P.M.B 65, Minna, Niger State, Nigeria,*
verathomas081@gmail.com

[4] *Department of Agricultural &Bioresources Engineering, Federal University of Technology, Minna, Niger State, Nigeria,*
oshatoladavid@gmail.com

[5] *Department of Agricultural &Bioresources Engineering, Federal University of Technology, Minna, Niger State, Nigeria,*
idrismusa109@gmail.com

***Corresponding Author:** *Gana Ibrahim Mohammed;* ganaibro74@yahoo.com

Manuscript History
Received: 16/03/2026
Revised: 15/04/2026
Accepted: 30/04/2026
Published: 05/05/2026
https://doi.org/10.5281/zenodo.20075997

Abstract: *Traditional fufu production from cassava is labour-intensive, time-consuming, and often characterised by poor hygiene and limited scalability, necessitating mechanised alternatives. This study aimed to design, fabricate, and evaluate the performance of a motorized cassava dough (fufu) processing machine to improve productivity, consistency, and operational safety. The machine, comprising a frame, hopper, stainless steel beaters, bevel gear system, belt–pulley arrangement, and a 6.5 hp petrol engine, was developed using standard mechanical engineering design procedures, with a power requirement of 4.77 kW. Performance evaluation was conducted using a three-factor Central Composite Rotatable Design under Response Surface Methodology, considering cassava mass (13–46 kg), pounding speed (395–1405 rpm), and processing time (3–24 min). The results showed that machine capacity ranged from 85.2 to 126.74 kg h⁻¹, while pounding efficiency varied between 78.5% and 94.51%. Optimal conditions were obtained at 40 kg batch mass, 1200 rpm, and 20 min, yielding a capacity of 126.74 kg h⁻¹ and efficiency of 94.51%. The study demonstrates that optimisation of processing parameters significantly enhances machine performance and product quality. Further research should focus on alternative energy sources, durability assessment, and automation improvements to enhance large-scale adoption.*

Keywords: *Cassava Processing, Fufu Machine, Machine Capacity, Pounding Efficiency, Response Surface Methodology, Speed Optimization*

INTRODUCTION

Cassava (Manihot esculenta Crantz) is a major staple root crop cultivated extensively across tropical and subtropical regions, particularly in Africa, Asia and Latin America. Owing to its tolerance to drought, adaptability to marginal soils and relatively high yield per unit area, cassava plays a critical role in global food security. It is estimated to provide dietary energy for more than 800 million people worldwide (FAO, 2013). In sub-Saharan Africa, cassava is not only a subsistence crop but also a strategic commodity for poverty alleviation and rural livelihoods. The crop is processed into numerous traditional food products, including garri, tapioca and fufu, which contribute significantly to household nutrition and income generation (Sanni *et al*., 2024). Fufu is a fermented or boiled cassava-based dough widely consumed in West and Central Africa. It is typically prepared by boiling cassava roots and pounding them sometimes in combination with plantain or yam until a smooth, cohesive and elastic texture is achieved. The product is commonly served with soups and stews and occupies an important cultural and dietary position in many communities (Afoakwa *et al*., 2020). Despite its importance, traditional fufu preparation remains labour-intensive, time-consuming and physically demanding. The pounding operation is usually carried out manually using a mortar and pestle, requiring considerable effort, coordination and skill to obtain the desired consistency (Oyeyinka & Oyeyinka 2018). In addition to labour demands, the traditional method presents challenges related to hygiene, product uniformity and limited production scale. The increasing demand for cassava-based foods in urban centres, coupled with the need to improve processing efficiency and product quality, has intensified interest in mechanised solutions. Mechanisation of traditional food processing operations has been shown to enhance productivity, reduce drudgery and improve sanitary conditions. Although mechanised systems have been developed for related operations, such as yam pounding, many existing designs are constrained by high energy requirements, inadequate texture control, high fabrication costs and limited durability (Adesuyi *et al.* 2024). These limitations highlight the need for improved cassava dough processing equipment that balances performance, cost-effectiveness and operational reliability. Therefore, the development of a motorised cassava dough (fufu) processing machine represents an important step towards modernising traditional food systems. Such innovation seeks to enhance processing capacity, ensure consistent product quality, reduce human labour and support small- and medium-scale enterprises, while preserving the cultural relevance of fufu consumption. This study contributes to ongoing efforts in agro-processing mechanisation by designing, fabricating and evaluating a machine intended to provide a hygienic, efficient and economically viable alternative to manual pounding methods

MATERIALS AND METHODS

2.1 Machine Descriptions

The motorised cassava dough (fufu) processing machine was designed and fabricated using locally available materials. The major components include the frame (Fig. 1), hopper, pounding unit assembly (Fig. 2), gearbox (Fig. 3), belt–pulley system, and a 6.5 hp petrol engine. The frame was constructed from mild steel angle iron to provide structural rigidity and support for all machine components. The hopper serves as the processing chamber and houses the rotating stainless-steel beaters, which are mounted on a vertical shaft. The pounding unit operates by shearing and compressing boiled cassava to produce a smooth and cohesive dough. Power transmission is achieved through a belt–pulley arrangement connected to a gearbox containing bevel gears, which convert horizontal motion from the engine to vertical motion required for pounding.



Fig. 1 Machine Frame Fig. 2 Assembled Machine Fig. 3 Gear Box

2.2 Design Analysis

The following design calculations were carried out.

1. Determination of Drum (hopper) dimensions

The hopper's volume was determined as follows as reported by Shigley *et al.* (2011);

$$V_{hp} = \frac{m_f}{\rho_f} \quad (1)$$

$$V_{hp} = \pi r^2 h_c \quad (2)$$

Where, V_{hp} is the volume of the hopper (m^3), m_f is the mass of (fufu) to be pound (kg) (assuming 40 kg per batch), ρ_f is the density of fufu (kg/m^3), r is the radius of the container (m), h_c is the height of the container (m), π is constant (3.142),

2.3 Powertrain of the Machine

The power train of the fufu-making machine starts with the petrol engine, which drives a pulley connected by a belt to a pulley on the horizontal shaft; the horizontal shaft then transmits motion into a gearbox containing bevel gears that redirect the rotation from horizontal to vertical, and this vertical shaft finally rotates the beaters inside the hopper to pound the fufu. The Process diagram of the machine powertrain is presented in Fig. 4 and the power train in the gearbox is shown in Fig. 5.

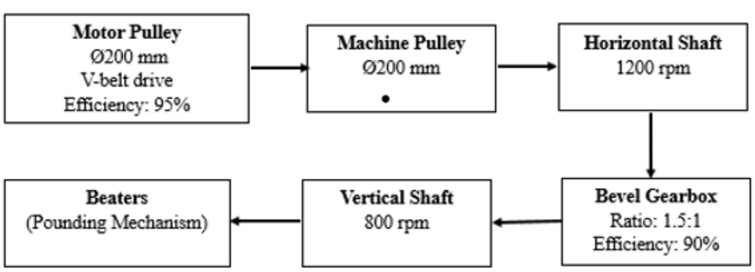

Fig. 4. The process diagram of the machine powertrain

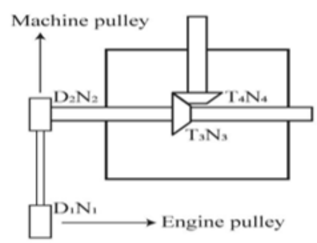

Fig. 5. Power Train in the gearbox

2.4 Determination of the Gear Ratio

The gear ratio was determined using the relationship reported by Khurmi and Gupta, (2005), and is given as

$$G.R = \frac{T_V}{T_h} \quad (3)$$

Where, G.R is the gear ratio, T_V is the number of Teeth on Vertical Bevel Gear, T_h is the Number of Teeth on Horizontal Bevel Gear.

2.5 Determination of the Shafts Speed

There are two shafts in the machine power train; horizontal shaft and vertical shaft

Determination of the Horizontal Shaft Speed

The speed of the horizontal shaft (N_V) was determined as reported by Khurmi and Gupta, (2005), and is given as

$$N_2 = N_1 . \frac{D_1}{D_2} \quad (4)$$

Where, N_2 is the horizontal shaft speed (rpm), N_1 is the electric motor speed (rpm), D_2 is the horizontal shaft pulley diameter (m), D_1 is the electric motor shaft pulley diameter (m),

Determination of the Vertical Shaft Speed

Using the gear ratio, the speed of the vertical shaft (N_V) was determined as reported by Khurmi and Gupta, (2005), and is given as

$$N_V = N_h . \frac{T_h}{T_v} \quad (5)$$

Where, N_h is the horizontal shaft speed (rpm), N_v is the vertical shaft speed (rpm), T_h is the number of teeth on the horizontal shaft, T_v is the number of teeth on the vertical shaft

Determination of Torques in the Horizontal and Vertical Shafts

The torques in the shafts were determined as reported by Khurmi and Gupta, (2005), and is given as

Torque on Vertical Shaft

$$T_V = F_S \times r_c \quad (6)$$

$$F_S = (M_f + M_{hs} + M_{vs} + M_p + M_{gb}) \times g \quad (7)$$

Where, T_V is the torque on vertical shaft (Nm), r_c is the crank radius (m), M_f is the mass of fufu (kg), M_{hs} is the mass of horizontal shaft (kg), M_{vs} is the mass of vertical shaft (kg), M_p is the mass of pulley (kg), M_{gb} is the mass of the gearbox (kg), g is the acceleration due to gravity (9.81 m/s^2)

2.6 Power Required by the Machine

The power required by the machine was determined as reported by Khurmi and Gupta, (2005), and is given as

$$P_T = \left[\frac{2\pi N T_V}{60}\right] \quad (8)$$

Where P_T is the total power required (kW), T_v is the total torque on the vertical shaft (Nm), N the rotational speed (rpm), π is constant,

2.7 Determination of Diameter of the Shaft

The shaft diameter is designed based on the combined bending and torsional stresses using the ASME code equation, reported by was determined as reported by Khurmi and Gupta, (2005), and is given as:

$$d^3 = \frac{16}{\pi S_s}\sqrt{(K_b M_b)^2 + (K_t M_t)^2} \quad (9)$$

$$M_b = m \times g \times L \quad (10)$$

where, d is expected diameter of shaft(m), M_t is belt moment (Nm), M_b is bending moment (Nm), K_b is shock and fatigue factor applied to bending moment, K_t is shock and fatigue factor applied to torsional moment, S_S is permissible shear stress of the shaft, M_b is the bending moment (Nm), g is the acceleration due to gravity, L is the length of the shaft (m)

2.8 Determination of Torques on the Horizontal and Vertical Shafts

The torques on the shafts were determined as reported by Khurmi and Gupta, (2005), and is given as

Torque on Vertical Shaft.

The vertical shaft torque comes from the direct gravitational load acting through the crank radius, while the horizontal shaft torque is a transmitted torque that depends on the gear ratio.

$$T_V = F_S \times r_c \quad (11)$$

$$F_S = (M_f + M_{hs} + M_{vs} + M_p + M_{gb}) \times g \quad (12)$$

Where, T_V is the torque on vertical shaft (Nm), r_c is the crank radius (m), M_f is the mass of fufu (kg), M_{hs} is the mass of horizontal shaft (kg), M_{vs} is the mass of vertical shaft (kg), M_p is the mass of pulley (kg), M_{gb} is the mass of the gearbox (kg), g is the acceleration due to gravity (9.81 m/s²)
Torque on Horizontal Shaft

$$T_h = \frac{T_v}{G.R} \quad (13)$$

Where, T_h is the torque on horizontal shaft (Nm), T_V is the torque on vertical shaft (Nm), G.R is the gear ratio
Power Required by the Machine
10. Determination of machine pulley diameter
Using the relationship stated in Khurmi and Gupta (2005), the machine pulley's diameter was calculated and is provided as

$$N_1 . D_1 = N_2 . D_2 \quad (14)$$

$$D_2 = \frac{N_1 . D_1}{N_2} \quad (15)$$

Where, N_1 is the speed of the petrol engine (rpm), D_1 is the diameter of the petrol engine pulley was already fixed on the engine (m), N_2 is the speed of the machine (rpm), D_2 is the diameter of machine pulley (m)

2.9 Determination of the Belt Speed
The belt speed was determined as follows

$$v = \frac{(\pi \times D_1 \times N_1)}{60} \quad (16)$$

Where, v is the belt speed of the machine (m/s), D_1 is the diameter of engine pulley (m), N_1 is the speed of the engine (rpm), π is the constant

Determination of Effective Belt Tension
The effective belt tension was determined as follows

$$T_e = \frac{P}{v} \quad (17)$$

Where, T_e is the effective belt tension (N), P is the power transmitted (watts), v is the belt speed (m/s)
The tension ratio was determined as

$$\frac{T_1}{T_2} = e^{(\mu \times \theta)} \quad (18)$$

$$\frac{T_1}{T_2} = e^{(0.3 \times \pi)} \quad (19)$$

Where, T_1 is the Tension in the tight side of the belt (N), T_2 is the tension in the slack side of the belt (N), μ is the coefficient of friction between the belt and pulley, θ is the angle of contact (wrap) on the pulley in radians, e is the Euler's number (≈ 2.718)

Determination of the Tight and Slack Side Tensions
The tight and slack tensions were determined as follows

$$T_1 - T_2 = T_e \quad (20)$$

Determination of Shaft Load Due to Belt
The load on the shaft due to the belt was determined as follows

$$F_{belt} = T_1 + T_2 \quad (21)$$

The Pulley Centre Distance
The pulley centre distance was determined as follows

$$C = 1.5 \times (D_1 + D_2) \quad (22)$$

Determination of belt length
The belt's length was calculated using the Khurmi and Gupta (2005) relationship, and it is provided as

$$L_T = 2C + \frac{\pi}{2}(D_2 + D_1) + \frac{(D_1 - D_2)^2}{4C} \quad (23)$$

where L_T is belt length (m), D_1 is diameter of electric motor's pulley (m), D_2 is diameter of machine pulley (m), C is the centre-to-centre spacing of the machine and electric motor pulley (m)

2.10 Determination of the Wrap Angle (θ)

The wrap angle on the smaller pulley was determined using an open belt drive formular

$$\theta = \pi - 2 \times \sin^{-1}\left(\frac{D_1 - D_2}{2 \times C}\right) \quad (24)$$

2.11 Determination of the Expected Slip

The slip in belt drives is typically estimated as:

$$\text{Slip} = \frac{((N_2 \times D_2) - (N_1 \times D_1))}{(N_2 \times D_2) \times 100} \quad (25)$$

2.12 Determination of Pitch Circle Radius

For spur gears, the pitch circle radius is related to the torque and force at the pitch circle: Assuming the force at the pitch circle is the same as the tangential force, and using torque on vertical shaft: The pitch circle radius was determined as follows:

$$T = F \times r_p \quad (26)$$

$$r_p = \frac{T}{F} \quad (27)$$

Where, r_p is the circle radius (m), F is force at the pitch circle (N), T is the torque at the pitch circle (Nm)

Pitch Circle Diameter

The pitch circle diameter was determined as follows

$$D = 2 \times r_p \quad (28)$$

Where, D is the circle diameter (m), rp is the circle radius (m),

Number of Teeth

The number of teeth was determined as follows

$$m = D/N \quad (29)$$

Where, m is the module (assume a standard module 0.004 mm), D is the diameter (m), N is the number of teeth

Outside Diameter

The outside diameter was obtained as follows

$$OD = D + 2m \quad (30)$$

Where, OD is the outside diameter (m) m is the module (m), D is the diameter (m), N is the number of teeth

Tangential Force on the Gear Teeth

The tangential force (F_t) acting on the gear teeth is calculated using the torque and pitch circle radius (r):

$$F_t = \frac{T}{r} \quad (31)$$

Determination of Radial Force on the Gear Teeth

The radial force (Fr) was calculated using the tangential force and pressure angle:

$$F_r = F_t \times \tan\emptyset \quad (32)$$

Where, F_r is the radial force (N), F_t is the tangential force (N), ∅ is the pressure angle (°)

2.13 Determination of the Load Bearing

The load bearing was determined as reported by Khurmi and Gupta (2005)

$$F_{max} = \frac{\sigma_y \times A}{FS} \quad (33)$$

$$A = \frac{\pi D}{4} \quad (34)$$

Where, F_{max} is the maximum load the shaft can bear (N), σ_y is the yield strength of the material (N/m^2), A is the cross-sectional area of the shaft (m^2), FS is the factor of safety (typically between 1.5 and 3), A is the area of the shaft (m^2), D is the shaft diameter (m)

2.14 Determination of Shear Stress on the Key

For rectangular keys under uniform shear, the shear stress on the key was determined as reported by Khurmi and Gupta (2005)

$$\tau = \frac{2 \times T}{d \times l \times h} \quad (35)$$

Where, τ is the shear stress (N/m^2), T is the torque (Nm), d is the shaft diameter (m), l is the key length (m), h is the height of the key (m)

2.15 Determination of Crushing Stress

The crushing stress was determined as reported by Khurmi and Gupta (2005)

$$\sigma_c = \frac{T}{d \times \frac{h}{2} \times l} \quad (36)$$

Where, σ_c is the crushing stress (〖N/m〗 ^2), T is the torque (Nm), d is the shaft diameter (m), l is the key length (m), h is the key height (m)

2.16 Bearing Selection

The bearing type was selection as recommended by International Organization for Standardization (IOS) (2017), a deep groove ball bearing suitable for radial and light axial loads was selected for the horizontal shaft. while an angular contact ball bearing designed to handle vertical thrust and radial loads was selected for the vertical shaft

Determination of Bearing Size and Load

The equivalent dynamic load was determined as reported by Khurmi and Gupta (2005).

$$P = X \times F_r + Y \times F_a \quad (37)$$

Where, P is the equivalent dynamic bearing load (N), F_r is the actual radial load on the bearing (N), F_a is the actual axial load on the bearing (N). This is the force acting parallel to the axis of rotation, X is the radial load factor (dimensionless), Y is the axial load factor (dimensionless).

Determination of L_{10} Life

Determination of Life cycle was determined as reported by SKF Group. (2023) follows

$$L_{10} = \left(\frac{C}{P}\right)^3 \times 10^6 \quad (38)$$

Where $\boldsymbol{L_{10}}$ is the Basic rating life (in revolutions), C is the Dynamic load rating (N), P is the equivalent dynamic bearing load, 10^6 is the Scaling factor to express life in millions of revolutions

Vibration Analysis

The First Critical Speed was determined as follows

$$N_C = \left(\frac{30}{\pi}\right) \times \sqrt{\frac{g}{\delta}} \quad (39)$$

$$\delta = \left(\frac{5 \times w \times L^4}{384 \times E \times I}\right) \quad (40)$$

$$I = \left(\frac{\pi \times d^4}{64}\right) \quad (41)$$

Where, N_C is the first critical speed (rpm), g is the acceleration due to gravity (m/s^2), δ is the static deflection of the shaft centre due to its own weight (m), w is the load per unit length (N/m), L is the length of shaft (m), E is the modulus of elasticity (N/m^2), for steel ≈ 2×10^{11} N/m^2), I is the moment of inertia

2.17 Mode of Operation

The machine operates by transmitting power from the petrol engine through a belt–pulley system to a gearbox, which drives the vertical shaft and attached beaters. Boiled cassava is introduced into the hopper, where it is subjected to continuous pounding action until a smooth dough consistency is achieved. Standard operating procedures (SOP) were followed, including pre-operation inspection, controlled loading within a capacity range of 13–46 kg, monitoring of processing time, and proper shutdown and cleaning to ensure hygiene and safety. A sample of the fufu produced by the machine is shown in Fig. 6.

Fig. 6. Sample of fufu pounded using the machine

2.18 Experimental Design Using Response Surface Methodology (RSM)

The performance evaluation of the machine was conducted using Response Surface Methodology (RSM) to investigate the effects of key operational variables and to optimise machine performance. A three-factor Central Composite Rotatable Design (CCRD) was employed. The independent variables considered were: cassava mass (X_1): 13–46 kg, pounding speed (X_2): 395–1405 rpm and pounding duration (X_3): 3–24 min. Each factor was varied at five levels (−α, −1, 0, +1, +α), where α = 1.682 to ensure rotatability of the design. The experimental design consisted of 20 runs, including 8 factorial points, 6 axial points, and 6 centre points to estimate experimental error and ensure model adequacy. The relationship between the independent variables and the responses was modelled using a second-order polynomial equation:

$$Y = \beta_0 + \sum\beta_i X_i + \sum\beta_{ii} X_i^2 + \sum\beta_{ij} X_i X_j \quad (42)$$

where: Yrepresents the predicted response (machine capacity or pounding efficiency), $\beta_0$is the intercept constant, $\beta_i$are the linear regression coefficients, $\beta_{ii}$are the quadratic regression coefficients; $\beta_{ij}$are the interaction regression coefficients, and $X_i$and $X_j$are the coded independent variables corresponding to the process factors.

2.19 Performance Evaluation Parameters

Machine Capacity

Machine capacity was defined as the quantity of cassava processed per unit time and was calculated as:

$$C_m = \frac{M_c}{t} \times 3600 \quad (43)$$

where, C_m is machine capacity (kg h⁻¹), $M_c$is mass of cassava processed (kg), t is processing time (s).

Pounding Efficiency

Pounding efficiency was determined as the ratio of properly processed cassava to the total cassava fed into the machine:

$$P_{EF} = \frac{M_{cp}}{M_{Tc}} \times 100 \quad (44)$$

where, P_{EF} is pounding efficiency (%), M_{cp} is mass of properly pounded cassava (kg), M_{Tc} is total mass of cassava fed (kg).

Statistical Analysis

Experimental data obtained were analysed using Design-Expert software (version 13) (Stat-Ease Inc., USA). Regression analysis was performed to fit the experimental data to the second-order polynomial model. The adequacy of the developed models was evaluated using: analysis of Variance (ANOVA) to determine the significance of model terms, coefficient of determination (R^2), adjusted R^2, and predicted R^2 to assess model fit , F-test and p-values ($p < 0.05$) to determine statistical significance and Lack-of-fit test to verify model adequacy. Response surface plots and contour plots were generated to visualise the interaction effects of process variables on machine performance. Numerical optimisation was carried out using the desirability function approach to determine the optimal combination of process parameters for maximum machine capacity and pounding efficiency. All experiments were conducted in triplicate at the centre points, and mean values were used for analysis to minimise experimental error.

2.20 Optimisation Procedure

Optimisation of the process variables was performed using the desirability function approach embedded in the RSM tool. The goal was to maximise both machine capacity and pounding efficiency simultaneously. The optimal conditions were selected based on the highest desirability value (close to 1), and the predicted optimum was validated experimentally to confirm the reliability of the model.

RESULTS AND DISCUSSION

The machine was designed, fabricated, and tested, with the test results summarized in Table-1. The machine's capacity ranged from 85.2 kg/h to 126.74 kg/h, while its pounding efficiency ranged from 78.5% to 94.51%. The lowest machine capacity of 85.2 kg/h, along with a pounding efficiency of 78.5%, was achieved using a combination of a 30 kg cassava mass, a pounding speed of 900 rpm, and a pounding duration of 3 minutes. In contrast, the highest machine capacity of 126.74 kg/h and a pounding efficiency of 94.51% were recorded with a combination of a 40 kg cassava mass, a pounding speed of 1200 rpm, and a pounding duration of 20 minutes.

Table-1 Results of performance testing of the machine

Std	Run	Mass of cassava (kg)	Speed of Pounding (rpm)	Pounding Duration (min)	Machine Capacity (kg/h)	Pounding Efficiency (%)
5	1	20	600	20	117.01	91.65
1	2	20	600	7	91.98	80.79
10	3	47	900	13.5	122.97	93.45
2	4	40	600	7	97.63	83.15
12	5	30	1405	13.5	114.6	90.27
9	6	13	900	13.5	112.42	90.16
8	7	40	1200	20	126.74	94.51
18	8	30	900	13.5	120.5	93.6
13	9	30	900	3	85.2	78.5
15	10	30	900	13.5	120.1	93.5
4	11	40	1200	7	107.21	87.34
7	12	20	1200	20	119.9	93.57
3	13	20	1200	7	97.27	84.2
17	14	30	900	13.5	121.3	93.8
16	15	30	900	13.5	119.8	93.2
6	16	40	600	20	118.7	91.5
19	17	30	900	13.5	120.5	93.6
20	18	30	900	13.5	120.1	93.5
11	19	30	396	13.5	100.78	85.13
14	20	30	900	25	124.5	94.3

3.1 Model Fitting and Statistical Analysis

The experimental data from the Central Composite Rotatable Design (CCRD) were fitted to second-order polynomial models to predict machine capacity and pounding efficiency. Model adequacy was evaluated using ANOVA, coefficient of determination (R^2), adjusted R^2, predicted R^2, and lack-of-fit tests. For machine capacity, the quadratic model was highly significant ($F(9,10) = 92.47$, $p < .001$), with a high R^2 of 0.944, indicating that 94.4% of variability was explained. The adjusted R^2 (0.924) and predicted R^2 (0.901) were in close agreement, confirming strong predictive ability. The lack-of-fit was not significant ($p = .243$), indicating a good fit. Similarly, the pounding efficiency model was significant ($F(9,10) = 76.15$, $p < .001$), with $R^2 = 0.931$, adjusted $R^2 = 0.908$, and predicted $R^2 = 0.882$, showing good agreement. The lack-of-fit was also not significant ($p = .312$). Overall, the results confirm that Response Surface Methodology effectively models and optimizes the performance of the cassava dough processing machine

3.2 Effects of Process Variables on Machine Capacity

Regression analysis indicated that cassava mass (X_1), pounding speed (X_2), and pounding duration (X_3) significantly influenced machine capacity ($p < .05$). Pounding speed had the highest F-value, making it the most influential factor.

Table-2 ANOVA for Machine Capacity

Source	Sum of Squares	df	Mean Square	F-value	p-value
Model	4821.37	9	535.71	92.47	< 0.001***
X_1 (Mass)	612.84	1	612.84	105.72	< 0.001***
X_2 (Speed)	1543.26	1	1543.26	266.41	< 0.001***
X_3 (Time)	487.19	1	487.19	84.10	< 0.001***
X_1X_2	221.65	1	221.65	38.27	< 0.001***
X_1X_3	134.72	1	134.72	23.27	0.001
X_2X_3	198.55	1	198.55	34.27	< 0.001***
X_1^2	312.44	1	312.44	53.94	< 0.001***
X_2^2	721.83	1	721.83	124.63	< 0.001***
X_3^2	189.89	1	189.89	32.78	< 0.001***
Residual	57.94	10	5.79		
Lack of Fit	37.52	5	7.50	1.87	0.243
Pure Error	20.42	5	4.08		
Total	4879.31	19			

Model Summary:

$R^2 = 0.944$, Adjusted $R^2 = 0.924$, Predicted $R^2 = 0.901$

Table-3 ANOVA for Pounding Efficiency

Source	Sum of Squares	Df	Mean Square	F-value	p-value
Model	612.53	9	68.06	76.15	< 0.001***
X_1 (Mass)	72.44	1	72.44	81.06	< 0.001***
X_2 (Speed)	185.63	1	185.63	207.78	< 0.001***
X_3 (Time)	91.25	1	91.25	102.13	< 0.001***
X_1X_2	38.17	1	38.17	42.73	< 0.001***
X_1X_3	27.56	1	27.56	30.83	< 0.001***
X_2X_3	31.49	1	31.49	35.24	< 0.001***
X_1^2	54.62	1	54.62	61.14	< 0.001***
X_2^2	73.88	1	73.88	82.75	< 0.001***
X_3^2	37.49	1	37.49	41.99	< 0.001***
Residual	8.94	10	0.89		
Lack of Fit	4.73	5	0.95	1.54	0.312
Pure Error	4.21	5	0.84		
Total	621.47	19			

Gbabo *et al.*, (2026). Development and Performance Evaluation of a Motorized Cassava Dough Processing Machine. *Nigerian Journal of Engineering Science Research (NIJESR).*, 9(1), 59-71. https://doi.org/10.5281/zenodo.20075997

Model Summary:
R^2 = 0.931, Adjusted R^2 = 0.908, Predicted R^2 = 0.882
Capacity increased with cassava mass and processing time up to an optimum, after which overloading reduced performance. Similarly, increasing speed enhanced capacity due to higher shear and impact forces, but excessive speeds caused slight declines due to inefficiencies. Pounding duration also improved capacity, though gains became marginal beyond the optimum due to diminishing returns.

3.3 Response Surface of Effects of Pounding Time on Machine Capacity
Machine capacity depended on pounding time, cassava mass, and their interaction. Capacity rose from 90 kg/h to 118 kg/h as time increased from 7 to 15 minutes, with a slight increase to 120 kg/h at 20 minutes. While optimal time improves throughput, excessive duration reduces efficiency, consistent with Van der Sman (2020), who reported that prolonged processing lowers efficiency. Cassava mass also affected capacity, increasing from 90 kg/h to 108 kg/h as mass rose from 20 kg to 40 kg. However, excessive mass caused overloading and inefficiencies. This agrees with Singh and Heldman (2014), who emphasized optimal material loading, and Shigley *et al.* (2004), who highlighted the need to operate within design limits.

3.4 Response Surface of Effects of Pounding Speed on Machine Capacity
Capacity increased from 105 kg/h to 120 kg/h as speed rose from 600 rpm to 1000 rpm, but declined to 113 kg/h at 1200 rpm. This shows that optimal speed maximizes throughput, while excessive speed reduces efficiency due to incomplete processing, energy losses, and mechanical stress. Lower speeds also reduce capacity due to slower processing. This aligns with Adejumo and Ola (2012), who reported that higher speeds improve machine capacity by increasing processing rate.

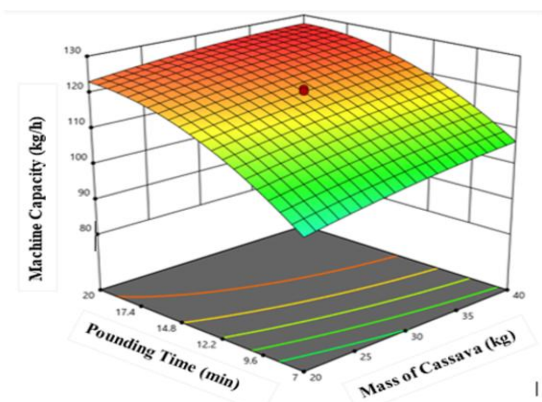

Fig. 6 Effects of Pounding Time and Mass of Cassava on Machine Capacity

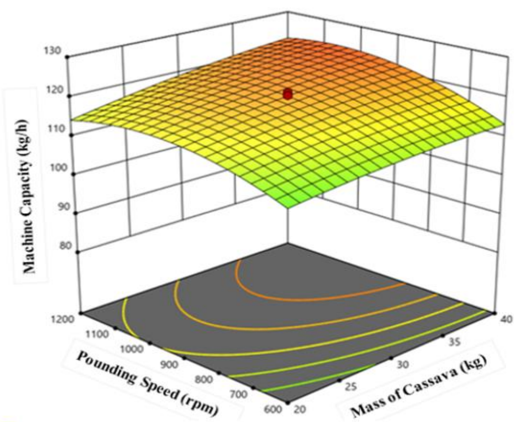

Fig. 7 Effects of Pounding Speed and Mass of Cassava on Machine Capacity

3.5 Effects of Process Variables on Pounding Efficiency
The analysis showed that all three variables significantly influenced pounding efficiency ($p < .05$), with pounding speed being the most dominant factor. Efficiency increased with processing duration, rising markedly between 7 and 20 minutes due to more complete breakdown of cassava particles, though gains beyond this range were minimal. Cassava mass exhibited a quadratic effect, with moderate loads (30–40 kg) yielding optimal efficiency, while low masses underutilized machine capacity and high masses caused overloading and incomplete pounding..

3.6 Response Surface of Effects of Effects of Pounding Time on Efficiency
The Pounding time improved efficiency from 83% to 93% between 7 and 15 minutes, with only slight gains to 94.5% at 20 minutes. However, excessive durations led to diminishing returns due to increased energy consumption and mechanical wear, while insufficient time resulted in incomplete processing. This agrees with Benton and Bailey (2019), who noted that optimizing processing time enhances food system efficiency.

3.7 Response Surface of Effects of Cassava Mass on Pounding Efficiency

Pounding Cassava mass increased efficiency from 83% to 87% as it rose from 20 kg to 40 kg, confirming that optimal batch size improves energy utilisation and output quality. This supports Edeh *et al*., (2022), who emphasised that balanced input mass prevents inefficiencies from underloading or overloading..

3.8 Response Surface of Effects of Pounding Speed on Efficiency

Pounding speed improved efficiency from 93% at 600 rpm to 95% at 1000 rpm, then slightly declined to 94% at 1200 rpm. Low speeds produced poor-quality output and longer processing times, while excessive speeds caused uneven pounding, heat generation, and energy losses. This is consistent with Odigboh (1999), who highlighted the need for optimal speed to balance efficiency, quality, and machine durability.

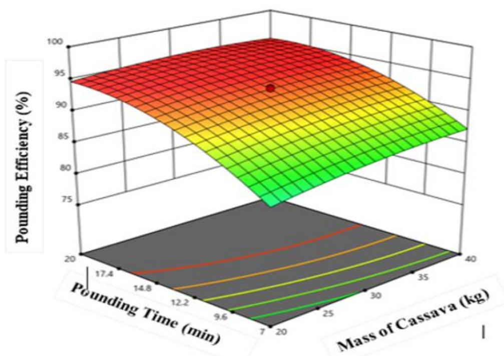

Fig. 8 Effects of Pounding Time and Mass of Cassava on Pounding Efficiency

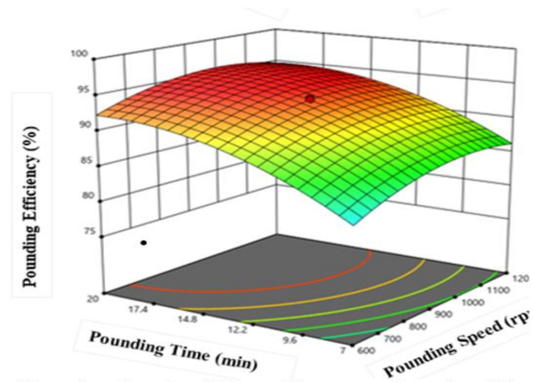

Fig. 9 Effects of Pounding Speed and Mass of Cassava on Pounding Efficiency

3.9 Optimisation and Model Validation

Numerical optimisation using the desirability function approach identified the optimal operating conditions as: cassava mass: 40 kg, pounding speed: 1200 rpm and pounding duration: 20 minutes. Under these conditions, the model predicted a machine capacity of 126.74 kg h^{-1} and pounding efficiency of 94.51%, with an overall desirability value close to 1.0. Experimental validation conducted under these optimal conditions produced results closely matching the predicted values, with deviations of less than 5%, confirming the adequacy and reliability of the developed models.

CONCLUSION

The motorised cassava dough processing machine was successfully designed, fabricated, and evaluated, demonstrating significant improvements in processing efficiency, productivity, and operational consistency compared to traditional methods. The study established that machine performance is strongly influenced by the combined effects of cassava mass, pounding speed, and processing duration, rather than by individual factors alone. The application of Response Surface Methodology (RSM) revealed significant linear, quadratic, and interaction effects of the process variables, underscoring the importance of parameter optimisation. The developed models showed high predictive capability, as indicated by strong coefficients of determination and non-significant lack-of-fit, confirming their suitability for process prediction and optimisation. Optimal operating conditions were identified at 40 kg cassava mass, 1200 rpm pounding speed, and 20 minutes processing time, yielding a maximum machine capacity of 126.74 kg h^{-1} and pounding efficiency of 94.51%. Operation within these optimal ranges enhances throughput, ensures product quality, and reduces energy losses and mechanical wear, while deviations from these conditions result in inefficiencies and potential machine overload. Overall, the findings validate RSM as an effective tool for modelling and optimisation of agro-processing equipment. The developed machine presents a viable, efficient, and scalable solution for cassava processing, with strong potential to support small- and medium-scale enterprises. Future research should focus on improving machine durability, reducing energy consumption, and integrating automation for enhanced performance and sustainability.

CONTRIBUTION TO KNOWLEDGE

This study developed a cost-effective motorised cassava dough processing machine that improves efficiency, reduces labour, and enhances product quality compared to traditional methods. It applied Response Surface Methodology (RSM) to model and optimise performance, producing reliable predictive models ($R^2 > 0.90$). The research identified optimal operating conditions (40 kg, 1200 rpm, 20 min) for maximum capacity and efficiency. It also revealed that machine performance depends largely on interaction effects of process variables. Overall, the work advances cassava processing technology, supports small-scale industrialisation, and provides a foundation for future improvements.

CONFLICT INTEREST

There is no conflict of interest for this research work.

REFERENCES

Adejumo, A. O., & Ola, F. A. (2012). Performance evaluation of a cocoyam peeling machine. *Journal of Agricultural Engineering and Technology*, *20*(2), 45–52.

Adesuyi, A. A., et al. (2024). Design challenges and performance limitations of mechanized food processing systems. *Journal of Food Engineering*, *350*, 111234

Afoakwa, E. O., Ismaila, S. O., Oyelami, A. T., & Shittu, T. A. (2020). Traditional processing and quality characteristics of fufu: A review. *African Journal of Food Science*, *14*(3), 65–78

Anas, A., Qutbuddin, S. M., Hebbal, S. S., & Kumar, A. C. (2012). An ergonomic study of work-related musculoskeletal disorders among workers in Indian sawmills. *International Journal of Engineering Research and Development*, *3*(9), 38–45

Benton, T. G., & Bailey, R. (2019). The impact of processing time on food system efficiency. *Food Policy*, *83*, 10–18.

Edeh, J. C., et al. (2022). Optimization of cassava processing parameters for improved efficiency. *Journal of Agricultural Processing Engineering*, *9*(1), 25–34.

Food and Agriculture Organization of the United Nations. (2013). *Save and grow: Cassava – A guide to sustainable production intensification*. FAO.

International Organization for Standardization. (2017). *Rolling bearings – Dynamic load ratings and rating life (ISO 281:2017)*. ISO.
Khurmi, R. S., & Gupta, J. K. (2005). *A textbook of machine design* (14th ed.). Eurasia Publishing House.

Odigboh, E. U. (1999). Machines for crop production. In *Agricultural mechanization in Nigeria*. University Press.

Oyeyinka, S. A., & Oyeyinka, A. T. (2018). A review on traditional processing of cassava and its products. *Food Reviews International*, *34*(6), 1–20.

Sanni, L. O., Adebowale, A. A., Awoyale, W., & Fetuga, G. O. (2024). Cassava utilization and food security in sub-Saharan Africa. *Journal of Root Crops*, *50*(1), 1–12.

Shigley, J. E., Mischke, C. R., & Budynas, R. G. (2011). *Mechanical engineering design* (9th ed.). McGraw-Hill.

Singh, R. P., & Heldman, D. R. (2014). *Introduction to food engineering* (5th ed.). Academic Press.

SKF Group. (2023). *Rolling bearings catalogue and life calculation guide*. SKF.

Van der Sman, R. G. M. (2020). Impact of processing conditions on food structure and quality. *Current Opinion in Food Science*, *35*, 85–91.